Chinese Chemical Letters 37 (2026) 111566

Contents lists available at ScienceDirect

Chinese Chemical Letters

journal homepage: www.elsevier.com/locate/cclet

Ratiometric fluorescence probe using semiconducting polymer nanoparticles and carbon dots for predicting anti-cancer efficiency

Tengfei Zhang[a], Chen Han[a], Chiyuan Wei[a], Xing Wang[a,c], Zhihui Jia[a], Hong-Min Meng[a,*], Zhaohui Li[a,b,*]

[a] College of Chemistry, Zhengzhou Key Laboratory of Functional Nanomaterial and Medical Theranostic, Zhengzhou University, Zhengzhou 450001, China
[b] The First Affiliated Hospital of Zhengzhou University, Zhengzhou 450052, China
[c] Engineering Chemistry and Testing Department, Sinopec Engineering (Group) Company Luoyang R&D Center of Technology, Luoyang 471003, China

ARTICLE INFO

Article history:
Received 18 January 2025
Revised 29 May 2025
Accepted 8 July 2025
Available online 9 July 2025

Keywords:
Immunogenic cell death
Damage-associated molecular patterns
ATP
Ratiometric fluorescence probe
Intracellular sensing

ABSTRACT

Immunogenic cell death (ICD) represents a specific form of tumor cell death that has the potential to elicit a tumor-specific immune response, resulting in a systemic anti-tumor effect and providing therapeutic benefits for metastatic lesions. The extensive research in this field has led to numerous studies confirming that during the induction of ICD, tumor cells can release damage-associated molecular patterns (DAMPs), which can be used as biomarkers to predict anti-cancer efficiency. However, few ratiometric fluorescent probes have been developed to tackle this fluctuation in living cells. In this study, we present a novel ratiometric fluorescence probe based on semiconducting polymer nanoparticles (SPNs) and carbon dots (CDs) for the sensing of DAMPs fluctuation in the ICD process by choosing adenosine triphosphate as a model. In this design, the fluorescence intensity of SPNs could not be affected by the change of target, while CDs could selectively respond to target, therefore realizing the ratiometric sensing of DAMPs. The ratiometric probe was successfully applied in real-time monitoring of the fluctuating concentration of DAMPs induced by doxorubicin in living cells. These results demonstrate that the ratiometric probe may become a promising agent for predicting anti-cancer efficiency.

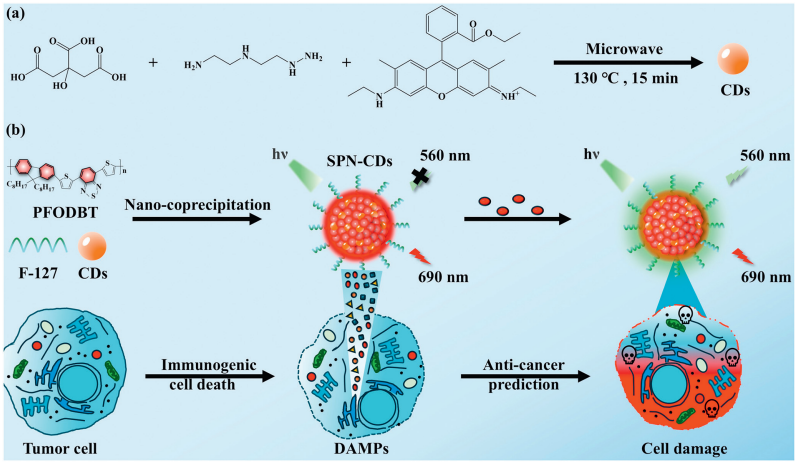
© 2025 Published by Elsevier B.V. on behalf of Chinese Chemical Society and Institute of Materia Medica, Chinese Academy of Medical Sciences.

Immunogenic cell death (ICD) is a highly effective method to stimulate the immunogenicity of cancer cells [1–3]. Some antitumor chemotherapeutic agents, such as doxorubicin (DOX), have the capacity to induce ICD in tumor cells, thereby facilitating the eradication of tumors [4–6]. Nevertheless, the inappropriate dosage of antitumor chemotherapeutic agents during cancer therapy remains a significant challenge that impedes the effective activation of the immune system against cancer through ICD. In particular, the low dose of the agent administered during treatment frequently results in insufficient ICD, whereas an excess of the agent may cause significant damage to adjacent normal tissues or immune cells [7–9]. Substantial research has demonstrated that during the induction of ICD, moribund tumor cells are capable of releasing damage-associated molecular patterns (DAMPs), including adenosine triphosphate (ATP), calreticulin (CRT), high mobility group box 1 (HMGB1), and heat shock protein (HSP) [10–12]. These DAMPs can stimulate the maturation of dendritic cells (DCs) and enhance the functionality of DCs for tumor-antigen recognition and presentation. Therefore, the detection of these DAMPs can significantly assist in prognostic immunotherapy assessments and minimize toxicity [13,14]. However, a highly specific imaging modality capable of visualizing the dynamic production of these DAMPs during cancer immunotherapy is both urgently needed and scarce.

Fluorescence imaging, which employs photon-electron interactions to elucidate biological processes, has become an indispensable tool for the detection of biomolecules in biological systems [15–17]. Despite significant advancements in the fluorescence probes, their detection modes mainly rely on the correlation between signal intensity at one channel and the analyte levels. This absolute intensity-dependent signal output may be easily affected by fluorescence intensity variations caused by the highly dynamic *in vivo* environment and the heterogeneous distribution of probes in tissues [18–21]. Therefore, fluorescence probes that use ratiometric measurement and offer a built-in self-calibration mechanism based on dual-channel fluorescence signal readout have been proposed [22–25]. Unlike single-emission sensors, which are susceptible to environmental variations (probe concentration and excitation intensity), ratiometric probes enable self-calibration. This significantly improves measurement accuracy and reliability.

* Corresponding authors.
E-mail addresses: hmmeng2017@zzu.edu.cn (H.-M. Meng), zhaohui.li@zzu.edu.cn (Z. Li).

https://doi.org/10.1016/j.cclet.2025.111566
1001-8417/© 2025 Published by Elsevier B.V. on behalf of Chinese Chemical Society and Institute of Materia Medica, Chinese Academy of Medical Sciences.



Scheme 1. (a) Synthesis route for CDs. (b) Schematic illustration of SPN–CDs synthesis and the mechanism for predicting anti-cancer efficiency.

Semiconducting polymer nanoparticles (SPNs) are fluorescent nanoparticles that exhibit high brightness, excellent photostability, as well as low toxicity, making them well-suited for applications in cell labeling and *in vivo* imaging [26,27]. In addition, thanks to their versatile surface modification, SPNs have also been used as biosensors for metal ions, glucose, and exosome sensing. Besides, previously we developed a biosensor based on SPNs for tumor imaging, demonstrating its great potential for bioimaging [28]. Hence, SPNs could be robust candidates to build novel ratiometric sensing systems. Moreover, as novel fluorescent nanomaterials, carbon dots (CDs) show excellent photostability, superior biocompatibility, and outstanding sensing ability, showing their great potential in bioimaging and biosensing [29–31]. Consequently, it is promising to prepare a ratiometric nanoprobe by rationally combining SPNs and CDs for DAMPs monitoring during ICD process.

In our previous study, we developed a highly sensitive and selective ATP probe based on CDs, which demonstrated excellent performance in both in buffer and cellular environments [32]. Moreover, poly[2,7-(9,9-dioctylfluorene)-alt-4,7-bis(thiophen-2-yl)benzo-2,1,3-thiadiazole] (PFODBT) is a semiconducting polymer nanoparticle known for its exceptional photostability, long-wavelength emission, and high fluorescence brightness, which remains unaffected by changes in the target analyte (ATP) [33]. Therefore, it is highly suitable to serve as the internal reference for our ratiometric nanoprobe. Here we present a novel ratiometric fluorescence probe SPN–CDs based on CDs and SPNs for the detection of DAMPs in the ICD process. ATP was chosen as a target model to investigate our design. As depicted in Scheme 1, SPN–CDs comprise PFODBT as an internal reference and CDs as the response domain because of their ability to respond to the target. In the presence of target, the fluorescence intensity of CDs at 560 nm increased obviously, while the emission peak of PFODBT at 690 nm remained unchanged. The variation of FL560/FL690 correlates directly with target content. The performance of this ratiometric fluorescence probe was finally demonstrated in DOX-treated tumor cells. SPN–CDs provided a simple and alternative parameter for predicting treatment outcomes in cancer chemotherapy.

Before the preparation of SPN–CDs, the feasibility of the proposed probe was first investigated. Here, CDs, which could respond to ATP specifically, were prepared by the microwave irradiation method. As shown in Figs. S1 and S2 (Supporting information), both the UV absorption peak of CDs at 540 nm and fluorescence emission peak at 560 nm increased with the increase of ATP concentration. The change of fluorescence intensity at 560 nm was shown in Fig. S3 (Supporting information), while the fluorescence emission peak of PFODBT at 690 nm remained unchanged with the variation of ATP concentrations (Fig. S4 in Supporting information). Based on this phenomenon, CDs were incorporated into PFODBT *via* encapsulation assisted by Pluronic F-127 to develop a ratiometric fluorescent nanoprobe for ATP sensing.

Before investigating the performance of SPN–CDs, experimental conditions were optimized. The doping ratio of CDs and PFODBT was first investigated. The concentration of PFODBT in SPN–CDs was maintained at 80 μg/mL, while CDs were changed (0.4, 0.6, 0.8, 1.0, 1.2 mg/mL) to prepare a series of SPN–CDs. These samples were then mixed with ATP at a consistent concentration. Although the concentration of CDs (1.2 mg/mL) exhibited the highest ratio of FL560/FL690, there was no significant increase in the FL560/FL690 ratio compared to 1.0 mg/mL (Fig. S5 in Supporting information). Additionally, considering the potential adverse effects of excessive particle size on cellular experiments, we chose 1.0 mg/mL CDs for subsequent experiments. Moreover, the ratio of FL560/FL690 at various reaction time points was also measured. As shown in Figs. S6 and S7 (Supporting information), the FL560/FL690 ratio increased over time, and plateaued at 15 min. Therefore, 15 min was chosen as the reaction time for subsequent experiments involving the interaction between the SPN–CDs and ATP. Subsequently, a series of characterizations were conducted on SPN–CDs. As seen from Fig. 1a, transmission electron microscopy (TEM) images demonstrate spherical morphology for these nanoparticles. Additionally, dynamic light scattering (DLS) measurements indicated an approximate hydrodynamic diameter of 51 nm (Fig. 1b). The UV absorption peak at 533 nm and fluorescence emission peak at 560 nm increased in the presence of 2 mmol/L ATP (Figs. 1c and d).

Under optimized conditions, SPN–CDs were introduced into Tris–HCl containing various concentrations of ATP (ranging from 0 to 2.0 mmol/L) for quantitative analysis. As seen from Figs. 2a and b, with the ATP concentration increasing incrementally, the fluorescence intensity at 560 nm gradually increased, while the fluorescence intensity at 690 nm remained unchanged. Fig. 2c presented the linear relationship between the ratio of FL560/FL690 and ATP concentration. Within the ATP concentration range of 0.2 mmol/L to 0.8 mmol/L, a linear correlation ($R^2 = 0.9928$) was observed. The linear regression equation derived from this range is $y = 19.46x$ - 3.044 (where y represents the fluorescence ratio, and x represents the concentration of ATP). The limit of detection (LOD) was determined by the $3\sigma/k$ criterion and was calculated to be 21 μmol/L. In addition, the ability of SPN–CDs to bind specifically to ATP was also important. SPN–CDs were evaluated against a range of species for selectivity towards ATP. The fluorescence ratio of FL560/FL690 was observed to increase with the addition of ATP, while the addition of other competing molecules did not lead to an obvious change in

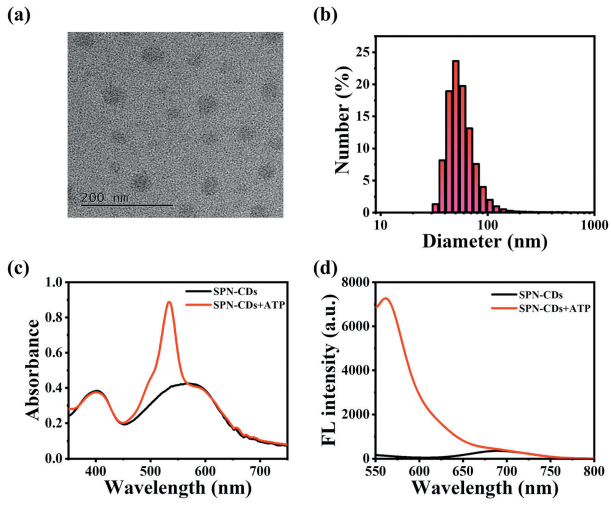


Fig. 1. (a) Transmission electron microscopy images of SPN–CDs. (b) Dynamic light scattering of SPN–CDs. (c) Absorption spectra of SPN–CDs (80 μg/mL PFODBT, 1 mg/mL CDs) with 2 mmol/L ATP. (d) Fluorescence spectra of SPN–CDs (80 μg/mL PFODBT, 1 mg/mL CDs) with 2 mmol/L ATP.

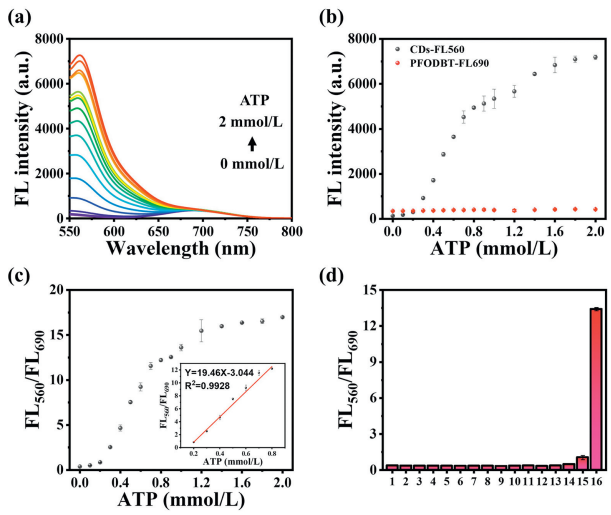


Fig. 2. (a) Fluorescence spectra of SPN–CDs (80 μg/mL PFODBT, 1 mg/mL CDs) with ATP (0–2 mmol/L). (b) Fluorescence intensity of SPN–CDs (80 μg/mL PFODBT, 1 mg/mL CDs) with ATP (0–2 mmol/L) at 560 nm and 690 nm. (c) The ratio of the FL560/FL690 of SPN–CDs with ATP (0–2 mmol/L). (d) Specificity assay of SPN–CDs with various species (1 mmol/L): 1, L-Leu; 2, L-Asp; 3, L-Val; 4, L-Thr; 5, L-Ser; 6, L-Pro; 7, DL-Phe; 8, DL-Try; 9, Met; 10, Na_2SO_4; 11, $Mg(NO_3)_2$; 12, NaCl; 13, KH_2PO_4; 14, UTP; 15, GTP; 16, ATP.

the fluorescence (Fig. 2d). The results indicate that SPN–CDs display excellent selective properties towards ATP. Importantly, even in the presence of a mixture of ATP and interfering substances, the FL560/FL690 ratio still reached levels comparable to those with ATP alone. These results confirm that SPN–CDs exhibit excellent selectivity for ATP and could accurately detect ATP in complex environments with multiple interfering substances (Fig. S8 in Supporting information).

The detection of ATP using fluorescent probes can be influenced by various factors, including probe concentration, laser power, probe stability, and physiological conditions. In this study, we evaluated the anti-interference capability of SPN–CDs during ATP detection under different conditions. As shown in Fig. S9 (Supporting information), when SPN–CDs (based on different PFODBT concentrations) were incubated with a constant ATP concentration, a consistent fluorescence ratio (FL560/FL690) was observed, indicating independence from probe concentration. In addition, the intensity of a single fluorescence signal was significantly affected by the laser voltage, so we tested the effect on the fluorescence signal ratio. Both FL560 and FL690 were proportional to voltage, while FL560/FL690 remained constant, underscoring the resilience of the probe against laser power variations (Fig. 3a). These findings demonstrate that the fluorescence ratio of SPN–CDs could mitigate potential interferences, enabling accurate ATP quantification in complex environments.

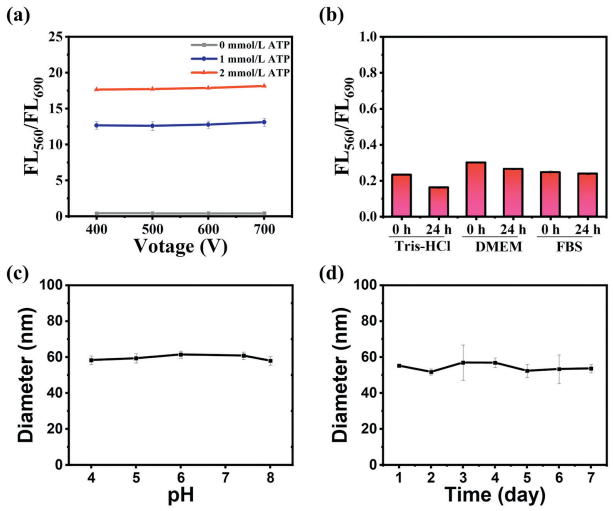


Fig. 3. (a) The ratio (FL560/FL690) change of SPN–CDs (80 μg/mL PFODBT, 1 mg/mL CDs) with 0, 1, 2 mmol/L ATP at different excitation voltages. (b) The change of ratio (FL560/FL690) of SPN–CDs (80 μg/mL PFODBT, 1 mg/mL CDs) in different buffer over 24 h. (c) The average dynamic light scattering of SPN–CDs (80 μg/mL PFODBT, 1 mg/mL CDs) at different pH values. (d) The average dynamic light scattering of SPN–CDs (80 μg/mL PFODBT, 1 mg/mL CDs) after 7 days of storage.

The robust stability of the nanoprobe in complex biological environments is crucial for cell experiments. Thus, their stability was thoroughly investigated. As depicted in Fig. 3b, SPN–CDs exhibited consistent luminescence properties after incubation in various buffer solutions for 24 h. The change of fluorescence intensity in different buffers was shown in Fig. S10 (Supporting information). As depicted in Fig. 3c, following the incubation of SPN–CDs in Tris–HCl buffer with diverse pH values, the particle sizes remained virtually unchanged. Moreover, it was observed that when SPN–CDs were continuously incubated in Tris–HCl buffer for a period of 7 days, the variation in particle size was negligible (Fig. 3d). This strongly indicates their outstanding stability and reliability within complex biological matrices.

To enable dynamic tracking of ATP within cells, establishing a reversible sensing system is critical. In this study, apyrase (an enzyme that hydrolyzes ATP to AMP) was employed to validate the reversibility. Experimental results demonstrated that introducing gradient concentrations of apyrase into CDs solution containing 1 mmol/L ATP induced a concentration-dependent fluorescence quenching of CDs (Fig. S11 in Supporting information). This time-dependent response confirms the reversible nature of ATP recognition, highlighting the potential of CDs for real-time ATP monitoring.

SPN–CDs exhibited excellent performance, including high anti-interference capability, robust stability, and high sensitivity toward ATP. This encouraged us to explore their cell imaging ability. The biological compatibility of SPN–CDs was first tested by MTT assay. SPN–CDs were incubated with MCF-7 and HeLa cells at different concentrations for 24 h at 37 °C, and the cell viability was still over 80 % (Figs. S12 and S13 in Supporting information). The results showed that the SPN–CDs had no apparent toxicity.

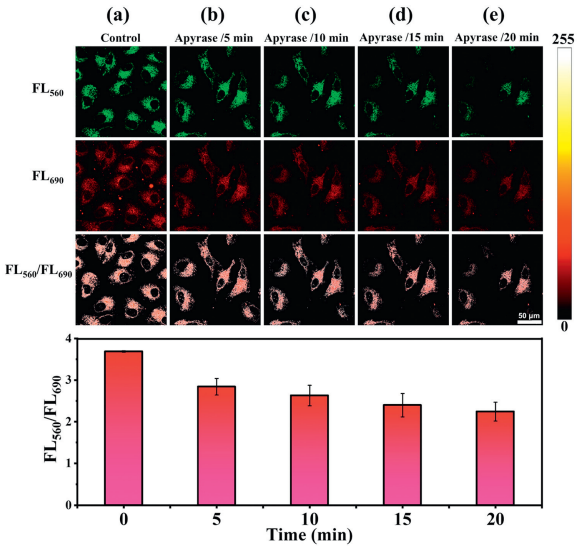


Fig. 4. Fluorescence images of SPN–CDs (200 μg/mL PFODBT, 2.5 mg/mL CDs) in MCF-7 cells incubated with apyrase for different time periods: (a) 0, (b) 5, (c) 10, (d) 15 and (e) 20 min. Scale bar: 50 μm.

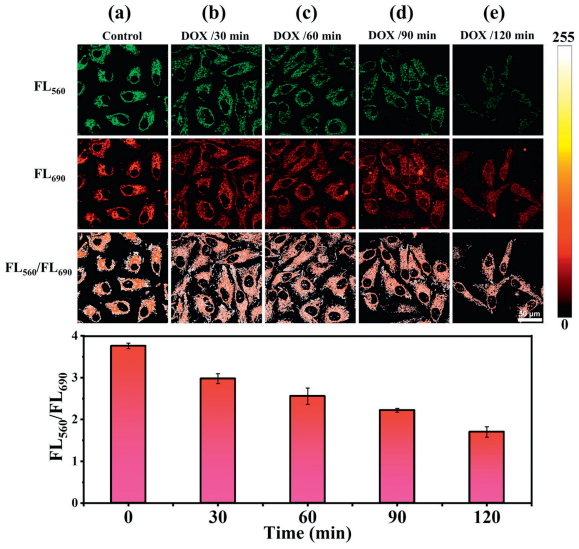


Fig. 5. Fluorescence images of SPN–CDs (200 μg/mL PFODBT, 2.5 mg/mL CDs) in MCF-7 cells incubated with DOX (2 μg/mL) for different time periods: (a) 0, (b) 30, (c) 60, (d) 90 and (e) 120 min. Scale bar: 50 μm.

Subsequently, to dynamically monitor intracellular ATP levels, we applied apyrase to MCF-7 cells pre-treated with SPN–CDs for 3 h (Fig. 4). Fluorescence images were obtained at 0, 5, 10, 15 and 20 min following the administration of the treatment. A decrease in the fluorescence ratio of FL560/FL690 was observed over time. The results further suggest that SPN–CDs were capable of dynamically monitoring changes in ATP levels in cells.

Most clinical chemotherapy drugs induce ICD, causing intracellular ATP to be released extracellularly when tumor cells undergo apoptosis. DOX, characterized by strong ICD induction, low-dose efficacy, and broad applicability across cancer types, can be utilized in cells to validate the detection efficacy of SPN–CDs for ATP release during ICD [34–36]. Hence, SPN–CDs were employed to monitor ATP production by cells during ICD induced by DOX. After adding DOX, the brightness of the FL560/FL690 ratio graph gradually decreased, indicating a reduction in intracellular ATP levels (Fig. 5). Hence, SPN–CDs prove to be an effective and reliable probe for sensitive imaging of intracellular ATP levels during ICD.

In summary, we developed a ratiometric fluorescence probe based on SPNs and CDs to visualize DAMPs in the ICD process. The designed ratiometric fluorescence probe possessed the following advantages: (1) Instead of relying on signal fluorescence intensity at one channel, the proposed probe is based on dual-channel fluorescence signals, exhibiting favorably accurate measurements; (2) such a probe possesses high anti-interference capability, resulting in intracellular high-fidelity sensing; (3) the probe demonstrates high photostability, thereby enabling extended observation periods under laser irradiation to observe the ICD process. More importantly, the modular design of SPN–CDs, with SPNs as a stable internal reference and CDs as the responsive unit, allows for future adaptation to detect other DAMPs or biomarkers by simply replacing the recognition element. Because of these advantages, we expect that this research will provide a trustworthy approach for facilitating further studies on drug action mechanisms and predicting anti-cancer efficiency.

Declaration of competing interest

The authors declare that they have no known competing financial interests or personal relationships that could have appeared to influence the work reported in this paper.

CRediT authorship contribution statement

Tengfei Zhang: Writing – original draft, Methodology, Formal analysis, Conceptualization, Validation, Investigation, Data curation. **Chen Han:** Validation, Investigation, Methodology, Formal analysis. **Chiyuan Wei:** Investigation, Validation, Formal analysis. **Xing Wang:** Methodology, Formal analysis, Investigation. **Zhihui Jia:** Investigation, Visualization, Formal analysis. **Hong-Min Meng:** Supervision, Funding acquisition, Conceptualization, Writing – review & editing, Project administration, Data curation. **Zhaohui Li:** Visualization, Supervision, Funding acquisition, Writing – review & editing, Validation, Resources.

Acknowledgments

This work was supported by the National Natural Science Foundation of China (Nos. 22374136, 22274143), the National Key Research and Development Program (No. 2023YFF0714402), the Natural Science Foundation of Henan Province (Nos. 232300421021, 242300421121), Key projects of the Joint Fund for Science and Technology of Henan Providence (No. 222301420007) and Henan Fundamental Research Leading Talent.

Supplementary materials

Supplementary material associated with this article can be found, in the online version, at doi:10.1016/j.cclet.2025.111566.

References

[1] M. Zhang, X. Jin, M. Gao, et al., Adv. Mater. 34 (2022) 2205701.
[2] X. Duan, C. Chan, W. Lin, Angew. Chem. Int. Ed. 58 (2019) 670–680.
[3] L. Wang, R. Guan, L. Xie, et al., Angew. Chem. Int. Ed. 60 (2021) 4657–4665.
[4] Y. Li, X. Liu, X. Zhang, et al., Chem. Commun. 57 (2021) 12087–12097.
[5] L. Zhang, N. Montesdeoca, J. Karges, et al., Angew. Chem. Int. Ed. 62 (2023) e202300662.
[6] R. Han, Q. Liu, Y. Lu, et al., Biomaterials 281 (2022) 121328.
[7] C. Li, L. Tu, Y. Xu, et al., Angew. Chem. Int. Ed. 63 (2024) e202406392.
[8] M. Jiang, J. Zeng, L. Zhao, et al., Nanoscale 13 (2021) 17218–17235.
[9] H.M. Abdel-Bar, A.A. Walters, Y. Lim, et al., Theranostics 11 (2021) 8738–8754.
[10] X.C. Deng, J.L. Liang, S.M. Zhang, et al., Adv. Mater. 36 (2024) 2405673.
[11] H. Deng, W. Yang, Z. Zhou, et al., Nat. Commun. 11 (2020) 4951.
[12] Z. Huang, Y. Wang, D. Yao, et al., Nat. Commun. 12 (2021) 145.

[13] Z. Gao, S. Jia, H. Ou, et al., Angew. Chem. Int. Ed. 61 (2022) e202209793.
[14] B. Ding, P. Zheng, F. Jiang, et al., Angew. Chem. Int. Ed. 59 (2020) 16381–16384.
[15] K. Fujita, Y. Urano, Chem. Rev. 124 (2024) 4021–4078.
[16] Y. Xue, J. Chi, B. Ning, et al., Chem. Eng. J. 498 (2024) 155132.
[17] E.A. Owens, M. Henary, G.E. Fakhri, et al., Acc. Chem. Res. 49 (2016) 1731–1740.
[18] Q. Fu, X. Yang, M. Wang, et al., ACS Nano 18 (2024) 3916–3968.
[19] S.H. Park, N. Kwon, J.H. Lee, et al., Chem. Soc. Rev. 49 (2020) 143–179.
[20] W. Zhou, J. Gong, S. Lu, et al., Chem. Eng. J. 492 (2024) 152332.
[21] L. Gui, K. Wang, Y. Wang, et al., Chin. Chem. Lett. 34 (2023) 107586.
[22] J. Han, X. Yue, J. Wang, et al., Chin. Chem. Lett. 31 (2020) 1508–1510.
[23] Y. Yang, M. Xia, H. Zhao, et al., ACS Sens. 3 (2018) 2278–2285.
[24] M. Li, J. Fan, H. Li, et al., Biomaterials 164 (2018) 98–105.
[25] M. Xie, J. Chen, Y. Wang, et al., Chin. Chem. Lett. 35 (2024) 108575.
[26] W. Hou, Y. Yuan, Z. Sun, et al., Anal. Chem. 90 (2018) 14629–14634.
[27] H. Chen, J. Yu, X. Men, et al., Angew. Chem. Int. Ed. 60 (2021) 12007–12012.
[28] D. Zhao, A. Zhou, X. Dong, et al., Theranostics 14 (2024) 5141–5151.
[29] J. Sun, Q. Wang, J. Yang, et al., Microchim. Acta 186 (2019) 402.
[30] J. Jana, H.J. Lee, J.S. Chung, et al., Anal. Chim. Acta 1079 (2019) 212–219.
[31] G. Zou, S. Chen, N. Liu, et al., Chin. Chem. Lett. 33 (2022) 778–782.
[32] X. Geng, Y. Sun, Y. Guo, et al., Anal. Chem. 92 (2020) 7940–7946.
[33] Y. Wang, G. Song, S. Liao, et al., Angew. Chem. Int. Ed. 60 (2021) 19779–19789.
[34] L. Galluzzi, A. Buqué, O. Kepp, et al., Nat. Rev. Immunol 17 (2017) 97–111.
[35] J. Fucikova, E. Becht, K. Iribarren, et al., Cancer Res. 76 (2016) 1746–1756.
[36] A.D. Garg, S. More, N. Rufo, et al., OncoImmunology 6 (2017) e1386829.